Progress In Electromagnetics Research, Vol. 119, 363–379, 2011

A NEW LOOK AT THE POINT TARGET REFERENCE SPECTRUM FOR BISTATIC SAR

J. J. Wu*, J. Y. Yang, Y. L. Huang, Z. Liu, and H. G. Yang

School of Electronic Engineering, University of Electronic Science and Technology of China, No. 2006, Xiyuan Ave, High-tech West Zone, Chengdu 611731, China

Abstract—Focusing bistatic synthetic aperture radar (SAR) data in frequency domain requires two-dimensional (2D) point target reference spectrum (PTRS). Loffeld's bistatic formula (LBF) and the Method of Series Reversion (MSR) have been introduced recently to compute PTRS of bistatic SAR. In this paper, firstly we generalize the original LBF (OLBF) by introducing the Doppler contribution functions of transmitter and receiver. Thus, OLBF and its derivatives (e.g., extended LBF) can be viewed as special forms of the generalized LBF with constant Doppler contributions. Based on this, secondly the ideal LBF (ILBF) with no computing error, except the error resulting from the principle of stationary phase, is also presented. The ILBF reveals that the theoretical PTRS of bistatic SAR consists of only two monostatic terms, but it does not include bistatic deformation term in comparison with OLBF. It supplies us with a target when we deduce the PTRS for bistatic SAR. Finally, to get the precise analytical PTRS for general bistatic SAR, an approximated ILBF (AILBF) is proposed. It expresses the Doppler contributions of the transmitter and receiver as power series and can approach the ILBF very well. AILBF can keep the precision as MSR and inherit a simple form from LBF. In addition, error limit for the validity of bistatic PTRS is also given. The results in this paper can be used to develop imaging algorithms for extreme bistatic (e.g., spaceborne/airborne) and high squint (e.g., bistatic forward-looking) cases.

Received 7 May 2011, Accepted 1 August 2011, Scheduled 16 August 2011

* Corresponding author: Junjie Wu (junjie_wu@uestc.edu.cn).

1. INTRODUCTION

Synthetic Aperture Radar (SAR) uses relative motion between an antenna and its target region to provide distinctive long-term coherent-signal variations that are exploited to obtain finer spatial resolution than that is possible with conventional beam-scanning means [1–6]. Bistatic SAR, with separate transmitter and receiver, has received considerable attention recently [7, 8]. Because of this bistatic characteristic, it has many benefits compared with its monostatic counterpart [9, 10].

Similar to monostatic case, bistatic SAR focusing could be carried out in azimuth frequency domain to speed up imaging [11–15]. Hence, the point target reference spectrum (PTRS) becomes the basis for those frequency domain imaging algorithms, such as range-Doppler, Chirp-Scaling [16] and Omega-k [11, 17, 18]. Unfortunately, in bistatic SAR, the azimuth modulation is more complicated than that in monostatic case: bistatic SAR range history has two square roots which result from distinct transmitter and receiver, which implies that it is difficult to compute the analytical PTRS of bistatic SAR directly by applying principle of stationary phase (POSP) [19–21].

Up to now, several methods to calculate bistatic SAR PTRS have been reported [22]. Different from numerical methods [24], analytical methods usually use POSP to get the spectrum. Two main spectrum models using POSP for bistatic SAR are the spectrum of Loffeld's bistatic formula (LBF) [19] and the Method of Series Reversion (MSR) [23]. LBF uses second-order Taylor expansion of slant range histories from the transmitter and receiver to calculate the points of stationary phase (PSP). Combining the two individual PSPs yields an approximated bistatic PSP. The method of the original LBF (OLBF) works well for many airborne and spaceborne bistatic SAR modes [25]. However, if the geometry configuration difference between the transmitter and receiver becomes considerable, as in hybrid spaceborne/airborne case, it will suffer from a significant degradation. An extended LBF (ELBF) has been reported in [26] to solve this problem. The method uses time-bandwidth-product (TBP) to form two constant factors to weigh the different contributions of the transmitter and receiver to the whole Doppler frequency. This method has good performance for hybrid spaceborne/airborne side-looking case [30]. Nevertheless, as both OLBF and ELBF do not consider the Doppler contributions properly enough, they are not suitable for every mode of bistatic SAR, especially for large squint cases.

Based on the view that the transmitting PSP should be equal to the receiving one, some improved methods were proposed to overcome

the problems of OLBF and ELBF. In [31, 32], a new ratio factor was solved to compute the Doppler frequency contributions. But the method neglected the squint angle variance during the synthetic aperture based on the narrow-beam assumption. In [33], to make the difference between the transmitting and receiving PSPs zero, two partial derivative equations were obtained to solve the Doppler contributions. However, the method in [33] can only take account of the contributions of the zeroth and first order Doppler frequencies (Doppler centroid and Doppler frequency modulated rate). This would lead to some degradation when the method is used in cases with extreme squint or forward-looking cases to some extent.

Due to the series form, it is not easy for MSR to be used for imaging algorithm deducing, especially for Chirp-Scaling and Omega-k algorithms.

In this paper, we try to model the Doppler contributions of the transmitter and receiver directly. A generalized LBF (GLBF) for bistatic SAR is presented, of which the OLBF and ELBF can be viewed as special examples. Based on this, a concise but implicit form of the ideal LBF (ILBF) is also deduced. It is briefer than any other PTRS of bistatic SAR [22], and can be viewed as a target function when we compute the PTRS of bistatic SAR, because it almost has no deducing error. After that, an explicit approximated ILBF (AILBF) which expresses the Doppler histories of the transmitter and receiver

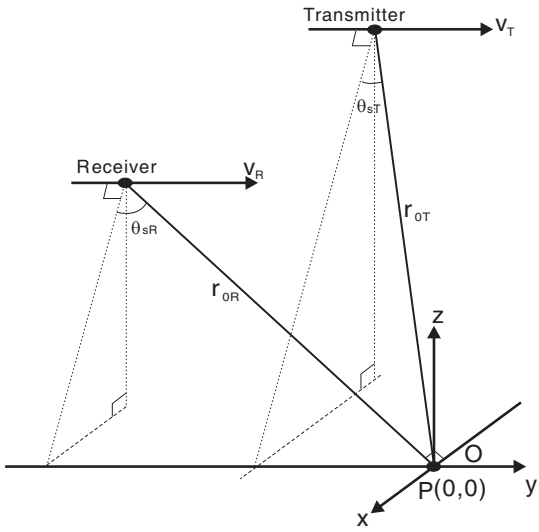

Figure 1. General geometry configuration of bistatic SAR at $\eta = 0$.

in ILBF as polynomial functions of the total Doppler frequency is presented. It can be used to focus general bistatic SAR, regardless of the bistatic and squint extent. Finally, we can find that, if we can model the Doppler contribution correctly, the AILBF and MSR can be unified. But AILBF has more precise style than MSR.

The rest of this paper is organized as follows: in Section 2, the proposed GLBF, ILBF, AILBF, and the error limit are presented. The numerical simulations are given in Section 3. And Section 4 concludes this paper.

2. 2D PTRS OF BISTATIC SAR

The geometry configuration of general bistatic SAR is shown in Figure 1. θ_s, v, and r_0 represent the squint angles, velocities and the center slant ranges of the transmitter (index T) and receiver (index R), respectively.

2.1. Bistatic SAR Signal Model

The range histories for the reference point target $P(0,0)$ of the transmitter and receiver are:

$$R_T(\eta) = \sqrt{r_{0T}^2 + v_T^2\eta^2 - 2v_T\eta\sin\theta_{sT}} \tag{1}$$

$$R_R(\eta) = \sqrt{r_{0R}^2 + v_R^2\eta^2 - 2v_R\eta\sin\theta_{sR}} \tag{2}$$

where η is the azimuth time variable.

The signal after demodulation to baseband and range Fourier transform is (constants are neglected):

$$S(f,\eta) = S_0(f)\exp\left\{-j2\pi(f+f_0)\frac{R_T(\eta)+R_R(\eta)}{c}\right\} \tag{3}$$

where f is the range frequency; $S_0(f)$ denotes the frequency spectrum of the transmitted signal; f_0 is the carrier frequency; c is the speed of light.

The 2D PTRS can be obtained by using POSP on azimuth:

$$S_{2df}(f,f_\eta) = S_0(f)\int\exp\{-j\phi_b(\eta,f_\eta)\}d\eta \tag{4}$$

where

$$\phi_b(\eta,f_\eta) = 2\pi\left\{\frac{f+f_0}{c}[R_T(\eta)+R_R(\eta)] + f_\eta\eta\right\} \tag{5}$$

and f_η is the azimuth frequency. To solve the above integration, bistatic PSP is required. Because two square root terms are involved in (5), it is difficult to obtain the analytical PSP directly.

2.2. GLBF

$\phi_b(\eta, f_\eta)$ can be divided into two parts corresponding to the transmitter and receiver, respectively:

$$\phi_T(\eta, f_{\eta T}) = 2\pi \left\{ \frac{f + f_0}{c} R_T(\eta) + f_{\eta T}(f_\eta)\eta \right\} \tag{6}$$

$$\phi_R(\eta, f_{\eta R}) = 2\pi \left\{ \frac{f + f_0}{c} R_R(\eta) + f_{\eta R}(f_\eta)\eta \right\} \tag{7}$$

where $f_{\eta T}(f_\eta)$ and $f_{\eta R}(f_\eta)$ are the Doppler frequencies assigned to the transmitter and receiver, respectively, and they are the functions of the total Doppler frequency.

Solving equations $\phi'_T(\eta, f_{\eta T}) = 0$ and $\phi'_R(\eta, f_{\eta R}) = 0$, we can get the following two PSPs $\hat{\eta}_{PT}(f_\eta)$ and $\hat{\eta}_{PR}(f_\eta)$:

$$\hat{\eta}_{PT} = \frac{r_{0T} \sin\theta_{sT}}{v_T} - \frac{c r_{0T} \cos\theta_{sT} f_{\eta T}(f_\eta)}{v_T^2 F_T} \tag{8}$$

$$\hat{\eta}_{PR} = \frac{r_{0R} \sin\theta_{sR}}{v_R} - \frac{c r_{0R} \cos\theta_{sR} f_{\eta R}(f_\eta)}{v_R^2 F_R} \tag{9}$$

where

$$F_T = \sqrt{(f + f_0)^2 - \left(\frac{c f_{\eta T}(f_\eta)}{v_T} \right)^2} \tag{10}$$

$$F_R = \sqrt{(f + f_0)^2 - \left(\frac{c f_{\eta R}(f_\eta)}{v_R} \right)^2} \tag{11}$$

Then by using the fact that the sum of two quadratic functions is a shifted and scaled quadratic function, bistatic PSP can be written as:

$$\hat{\eta}_{Pb} = \frac{\phi''_R(\hat{\eta}_{PR})\hat{\eta}_{PR} + \phi''_T(\hat{\eta}_{PT})\hat{\eta}_{PT}}{\phi''_R(\hat{\eta}_{PR}) + \phi''_T(\hat{\eta}_{PT})} \tag{12}$$

where

$$\phi''_T(\hat{\eta}_{PT}) = \frac{2\pi}{c} \frac{v_T^2}{r_{0T}\cos\theta_{sT}} \frac{F_T^3}{(f + f_0)^2} \tag{13}$$

$$\phi''_R(\hat{\eta}_{PR}) = \frac{2\pi}{c} \frac{v_R^2}{r_{0R}\cos\theta_{sR}} \frac{F_R^3}{(f + f_0)^2} \tag{14}$$

Substituting $\hat{\eta}_{Pb}$ into (5), we can obtain the final result of the bistatic PTRS:

$$S_{2df}(f, f_\eta) = S_0(f) \exp\{-j\Phi_{QM}(f, f_\eta)\} \times \exp\left\{ -\frac{j}{2}\Phi_{BD}(f, f_\eta) \right\} \tag{15}$$

where

$$\Phi_{QM}(f, f_\eta) = \phi_T(\hat{\eta}_{PT}) + \phi_R(\hat{\eta}_{PR}) \tag{16}$$

$$\Phi_{BD}(f, f_\eta) = \frac{\phi''_T(\hat{\eta}_{PT})\phi''_R(\hat{\eta}_{PR})}{\phi''_T(\hat{\eta}_{PT}) + \phi''_R(\hat{\eta}_{PR})}(\hat{\eta}_{PT} - \hat{\eta}_{PR})^2 \tag{17}$$

are the quasi-monostatic and bistatic deformation (BD) phase terms, respectively.

Equation (15) is the GLBF for bistatic SAR. Choosing different $f_{\eta T}(f_\eta)$ and $f_{\eta R}(f_\eta)$, we can obtain different forms of LBF. The OLBF assumes the Doppler contributions of the transmitter and receiver are equivalent. So $f_{\eta T}(f_\eta) = f_{\eta R}(f_\eta) = f_\eta/2$. The weighting method in [26] uses TBP as a factor to weigh the contributions of the transmitter and receiver to the common bistatic PSP. When the TBP is computed, the composite synthetic aperture time is used. So the weighting factor with TBP is also equal to the one with the azimuth frequency modulated rate. Hence, $f_{\eta T}(f_\eta)$ and $f_{\eta R}(f_\eta)$ are replaced by $f_{\eta rT}f_\eta/f_{\eta r}$ and $f_{\eta rR}f_\eta/f_{\eta r}$, respectively, where $f_{\eta rT}$, $f_{\eta rR}$ and $f_{\eta r}$ represent the Doppler frequency modulated rate of the transmitter, receiver and the total bistatic, respectively. So ELBF is also a special case of GLBF. In fact, the Doppler contributions can not be measured by the Doppler frequency modulated rates alone, especially in large squint cases, where the Doppler centroid $f_{\eta c}$ would be dominant in Doppler frequency [27–29]. So ELBF is just suitable for the cases of side-looking or low squint. As for large squint or forward-looking bistatic SAR [34], we should consider the influence of Doppler centroid sufficiently.

Now that Doppler contributions play such an important role in GLBF, what are the ideal Doppler contributions of the transmitter and receiver? And what can we get if we use the ideal Doppler contributions?

2.3. Ideal LBF

To evaluate the different contributions of the transmitter and receiver to the total bistatic Doppler frequency in PTRS, we should express $f_{\eta T}$ and $f_{\eta R}$ using f_η. Ideally the Doppler contributions of the transmitter and receiver can be written as:

$$\begin{aligned} f_{\eta T}(f_\eta) &= \frac{v_T \sin\theta_{sT}(f_\eta)(f + f_0)}{c} \\ f_{\eta R}(f_\eta) &= \frac{v_R \sin\theta_{sR}(f_\eta)(f + f_0)}{c} \end{aligned} \tag{18}$$

$\theta_{sT}(f_\eta)$ and $\theta_{sR}(f_\eta)$ represent the squint angles when the Doppler frequency is f_η. Then we have $F_T(f_\eta) = (f + f_0)\cos\theta_{sT}(f_\eta)$ and

$F_R(f_\eta) = (f + f_0)\cos\theta_{sR}(f_\eta)$. So the ideal PSP can be written as:

$$\eta_{PT} = \frac{r_{0T}}{v_T}\left[\sin\theta_{sT} - \cos\theta_{sT}\tan\theta_{sT}(f_\eta)\right] \tag{19}$$

$$\eta_{PR} = \frac{r_{0R}}{v_R}\left[\sin\theta_{sR} - \cos\theta_{sR}\tan\theta_{sR}(f_\eta)\right] \tag{20}$$

From the above expressions, we can find that the PSPs of the transmitter and receiver are the durations from the central Doppler time (beam-center) to the time when the whole Doppler frequency reaches at f_η. As for the transmitting and receiving stations, these two time lengthes should be the same. So theoretically η_{PT} is equal to η_{PR}.

Consequently, we can find that the BD phase term in (17) disappears. That is to say, different from the statement in [19], the ideal LBF does not need to include the BD phase term at all. This is a very important conclusion, which is beneficial to the analysis of signal properties of bistatic SAR and the development of the imaging algorithms, because the form of ILBF is similar to that of the monostatic case.

This result is based on the accurate modeling of the Doppler contributions of the transmitter and receiver. But it is very hard to get these models. Any approximation made in the modeling of the Doppler contributions would generate the difference between the PSPs of the transmitter and receiver, and then the BD phase term.

Next, to extend the application fields of LBF, we will deduce an approximated analytical form of the ILBF.

2.4. Approximated ILBF

In azimuth time domain, the precise Doppler frequency produced by the transmitter is:

$$f_{\eta T}(\eta) = -\frac{\left(v_T^2\eta - r_{0T}v_T\sin\theta_{sT}\right)(f + f_0)}{c\sqrt{r_{0T}^2 + v_T^2\eta^2 - 2r_{0T}v_T\eta\sin\theta_{sT}}} \tag{21}$$

and the Doppler frequency produced by the receiver is:

$$f_{\eta R}(\eta) = -\frac{\left(v_R^2\eta - r_{0R}v_R\sin\theta_{sR}\right)(f + f_0)}{c\sqrt{r_{0R}^2 + v_R^2\eta^2 - 2r_{0R}v_R\eta\sin\theta_{sR}}} \tag{22}$$

And the total bistatic Doppler frequency is $f_\eta(\eta) = f_{\eta T}(\eta) + f_{\eta R}(\eta)$.

From (21) and (22), we know if we want to get an accurate Doppler contribution relationship, we need to solve an eighth-order equation.

Here in this paper, considering the influence of the Doppler centroid, we express (21) and (22) as the following power series in η:

$$f_{\eta T} = f_{\eta cT} + f_{\eta rT}\eta + f_{\eta 3T}\eta^2 \dots \quad (23)$$

$$f_{\eta R} = f_{\eta cR} + f_{\eta rR}\eta + f_{\eta 3R}\eta^2 \dots \quad (24)$$

$$f_{\eta} = f_{\eta T} + f_{\eta R} = f_{\eta c} + f_{\eta r}\eta + f_{\eta 3}\eta^2 \dots \quad (25)$$

where the polynomial coefficients can be computed by Taylor expansion.

Eliminating η in (23) and (24) using (25), the relationships between $f_{\eta T}$, $f_{\eta R}$ and f_{η} are obtained:

$$f_{\eta T}(f_\eta) \approx f_{\eta cT} + \frac{f_{\eta rT}}{f_{\eta r}}(f_\eta - f_{\eta c}) - \frac{f_{\eta rT}f_{\eta 3} - f_{\eta 3T}f_{\eta r}}{f_{\eta r}^3}(f_\eta - f_{\eta c})^2 \dots \quad (26)$$

$$f_{\eta R}(f_\eta) \approx f_{\eta cR} + \frac{f_{\eta rR}}{f_{\eta r}}(f_\eta - f_{\eta c}) - \frac{f_{\eta rR}f_{\eta 3} - f_{\eta 3R}f_{\eta r}}{f_{\eta r}^3}(f_\eta - f_{\eta c})^2 \dots \quad (27)$$

These are the approximated contributions of the transmitter and receiver to the whole Doppler history and will be used to compute the bistatic PSP. Substituting the above two expressions into (8)–(17),

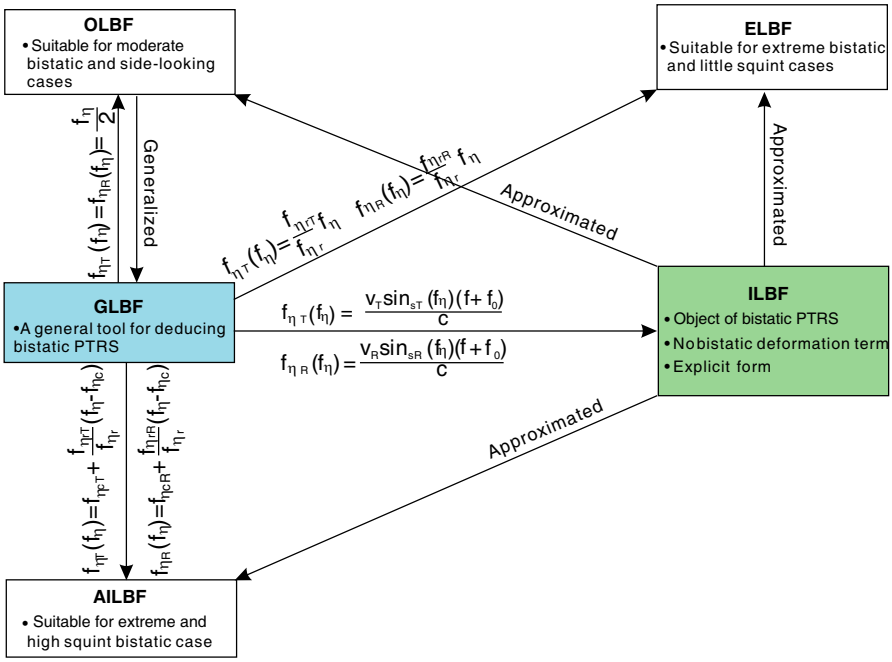

Figure 2. Relationships between OLBF, ELBF, GLBF, ILBF and AILBF.

we can get AILBF. It can be viewed as a more general form of LBF than OLBF, ELBF and other recently proposed forms in [31–33]. The result can be applied in hybrid spaceborne/airborne and high squint bistatic cases. Moreover, the accuracy of this method is "scalable" in the sense that its accuracy depends on the number of terms used in the power series. The performance of AILBF will be shown in Section 3.

Until now, we have mentioned five kinds of LBF: OLBF, ELBF, GLBF, ILBF and AILBF. The relationships between them are shown in Figure 2.

It is worth noting that, when we solve the Doppler contributions of the transmitter and receiver using (23), (24) and (25), we utilize a intermediate variable of azimuth time η. It is represented as a series function of f_η. This tells us that MSR and AILBF are unified in fact. They are both the approximation styles of ILBF, and their precisions are limited by the series order. After we get the series relationship between the azimuth time and Doppler frequency, if we use it directly to compute the PTRS, we will get the result of MSR. If the relationship is further used to model the transmitting and receiving Doppler frequencies, as (26) and (27), a PTRS of LBF style will be obtained. In practice, their precisions are the same. Consequently, AILBF can have the simple form like LBF and keep the precision of MSR at the same time.

3. ERROR LIMITS

In [22], a necessary condition which should be satisfied if OLBF can work well for some bistatic geometry configurations is presented. This condition judges the equivalence between the PSP of OLBF $\hat{\eta}_{Pb}(f_\eta)$ and the analytical one $\eta_{Pb}(f_\eta)$. Instead of evaluating the equality over all azimuth frequencies, the condition just considered the equivalence at the Doppler centroid: $\hat{\eta}_{Pb}(f_{\eta c}) \approx \eta_{Pb}(f_{\eta c})$.

However, when $\hat{\eta}_{Pb}(f_\eta)$ is just a shift result of $\eta_{Pb}(f_\eta)$, the imaging result is also a shift version of the ideal one according to the shift property of the Fourier Transform. Generally, this displacement does not influence the focusing performance. Therefore, we should not determine the geometry configuration limits related to PTRSs of kind LBF by just judging the equivalence between $\hat{\eta}_{Pb}(f_\eta)$ and $\eta_{Pb}(f_\eta)$, much less the equality between $\hat{\eta}_{Pb}(f_{\eta c})$ and $\eta_{Pb}(f_{\eta c})$.

In fact, the shape similarity between $\hat{\eta}_{Pb}(f_\eta)$ and $\eta_{Pb}(f_\eta)$ should be taken into account instead.

Here in this paper, we propose another method to determine the type of bistatic configurations that the PTRSs of sort LBF can focus:

$$\hat{\eta}_{Pb}(f_\eta) - \hat{\eta}_{Pb}(f_{\eta c}) \approx \eta_{Pb}(f_\eta) - \eta_{Pb}(f_{\eta c}) \tag{28}$$

The above equation means that, without considering the constant shift, the computed azimuth PSP should not have scale variation in comparison with the ideal one. And from (19) and (20), we know $\eta_{Pb}(f_{\eta c}) = 0$. So (28) can be simplified to:

$$\hat{\eta}_{Pb}(f_\eta) - \hat{\eta}_{Pb}(f_{\eta c}) \approx \eta_{Pb}(f_\eta) \tag{29}$$

Furthermore, the azimuth signal can be approximated as a linear frequency modulated signal generally. So the azimuth PSP is nearly linear with the Doppler frequency. Suppose the scale of $\hat{\eta}_{Pb}(f_\eta)$ compared with $\eta_{Pb}(f_\eta)$ is a. Then the quadratic phase error (QPE) resulting from the difference of PSP can be written as:

$$\Delta\phi_{\mathrm{QPE}} = \frac{\pi(1-a)^2 f_\eta^2}{f_{\eta r}} \tag{30}$$

The maximum QPE resulting from the difference of azimuth PSP can be written as:

$$\max \Delta\phi_{\mathrm{QPE}} = \frac{\pi(1-a)^2 (B_\eta/2)^2}{f_{\eta r}} \tag{31}$$

where B_η is the Doppler frequency bandwidth.

To avoid significant deterioration of the image quality, we would like to limit the maximum QPE to be within $\pi/4$ generally. If we limit $\max \Delta\phi_{\mathrm{QPE}}$ within $\pi/4$, we have:

$$1 - \frac{\sqrt{f_{\eta r}}}{B_\eta} < a < 1 + \frac{\sqrt{f_{\eta r}}}{B_\eta} \tag{32}$$

This condition can be viewed as a general necessary requirement which should be satisfied if the PTRSs of kind LBF, including the OLBF, ELBF and AILBF, can be applied to general bistatic cases.

4. SIMULATION RESULTS

In this section, we will compare the performance of OLBF, ELBF and AILBF. In addition, the influence of the expansion order on AILBF is also presented. The simulation parameters are shown in Table 1. The three cases differ in the squint and bistatic extent.

Case A is hybrid spaceborne/airborne forward-looking mode. The parameters of the spaceborne transmitter are accordant with those of TerraSAR-X. In this case, the airborne receiver works in forward-looking mode while the transmitter is little squint. In case B, both antennas are with medium squint angles. Finally, in case C we simulated the focusing performance of different LBFs for airborne bistatic forward-looking case.

Table 1. Simulation parameters.

Simulation parameters	Transmitter	Receiver
Center frequency	9.65 GHz	
Range Bandwidth	150 MHz	
PRF	Case A: 3500 Hz; Case B, C: 400 Hz	
Case A: Spaceborne/airborne (forward-looking)		
Range to point target	859 km	6.7 km
Velocity	7600 m/s	120 m/s
Squint/Downward-looking angle	-6.67°	27°
Case B: Airborne (medium squint)		
Range to point target	14.3 km	8.96 km
Velocity	120 m/s	120 m/s
Squint angle	8°	38°
Case C: Airborne (forward-looking)		
Range to point target	14.14 km	11.2 km
Velocity	120 m/s	120 m/s
Squint/Downward-looking angle	0°	27°

Negative squint angle means the antenna points backwards, and positive value means the antenna points forwards. Downward-looking angle is the angle between the receiver's line of sight and its moving direction.

4.1. Spectrum error and point target imaging results

Firstly, we compare the QPE of OLBF, ELBF and AILBF. Table 2 is the QPE between these PTRSs and the ideal spectrum. As for case A, if we use OLBF to compute the PTRS, the square root (11) is meaningless because of the incorrect Doppler assignment. So OLBF is invalid for squint spaceborne/airborne case. And the PSP scale of ELBF is nearly 1 while the QPE is less than $\pi/4$. So the focusing performance of ELBF for case A would not deteriorate obviously. But as for case B and C, the bistatic PSPs of both OLBF and ELBF have great variations from the ideal result and the QPEs also exceed the limitation of $\pi/4$. Then OLBF and ELBF will have poor abilities to focus the data of case B and C. But for AILBF, the PSP scale and QPE both have little deviations which can be neglected. So AILBF can be viewed as a proper approximation of ILBF.

Secondly, we use the ideal numerical PTRS, OLBF, ELBF and AILBF as matched filters for the method of 2D frequency domain

matching to focus the echo of a point target $P(0,0)$. Quality parameters, including impulse response width (IRW), peak sidelobe ratio (PSLR), and integration sidelobe ratio (ISLR), corresponding to case A-C are shown in Table 3.

From Table 3, it can be seen that for spaceborne/airborne forward-looking case, ELBF and AILBF both have a similar focusing ability with the ideal numerical spectrum. In the two airborne configurations, the imaging results of ELBF deteriorate with the growth of the squint extent. For case B with medium squint angles, the point target is poorly focused by using OLBF and ELBF, as shown in Figure 3. When the receiving antenna points to the forward-looking area in case C, ELBF can not focus on azimuth direction any more. However, from the simulation results, it can be seen that the results of AILBF agree

Table 2. Quadratic phase error of the three configurations.

		Scale a	QPE/π
Case A	OLBF	Invalid	Invalid
	ELBF	0.9596	-0.14
	AILBF	1	-4×10^{-4}
Case B	OLBF	0.8171	-2.1416
	ELBF	0.8221	-2.0256
	AILBF	1	-2.7456×10^{-9}
Case C	OLBF	0.4603	-11.9534
	ELBF	-0.3172	-71.2013
	AILBF	1	-2.1558×10^{-8}

Table 3. Quality parameters of the three configurations.

		IRW (Cells)	PSLR (dB)	ISLR (dB)
Case A	ANA	43.35	-13.27	-10.09
	OLBF	Invalid	Invalid	Invalid
	ELBF	47.54	-12.94	-9.99
	AILBF	43.39	-13.26	-10.09
Case B	ANA	25.24	-12.32	-10.15
	OLBF	186.3	Invalid	Invalid
	ELBF	158.43	Invalid	Invalid
	AILBF	25.27	-12.32	-10.15
Case C	ANA	37.43	-13.06	-10.14
	OLBF	Invalid	Invalid	Invalid
	ELBF	Invalid	Invalid	Invalid
	AILBF	37.45	-13.06	-10.14

well with the analytical results in these extreme bistatic configurations, like hybrid spaceborn/airborne and bistatic forward-looking cases.

4.2. The Influence of the Doppler Expansion Order

In this subsection, we will discuss the influence of the expansion order used in (26) and (27) on the approximation of ILBF.

Figure 4 illustrates the phase error and BD term of AILBF using 1st-order and 2nd-order expansions of the Doppler frequency for case C. They both increase with the range and azimuth frequencies. In Figures 4(a) and (b), the phase error is much less than $\pi/4$. So the precision can be guaranteed by using both 1st-order and 2nd-order expansions. However, the BD term using 1st-order expansion exceeds the maximum phase error limitation of $\pi/4$. So if we want to neglect the BD term for imaging algorithm development, we should use at least 2nd-order term in (26) and (27).

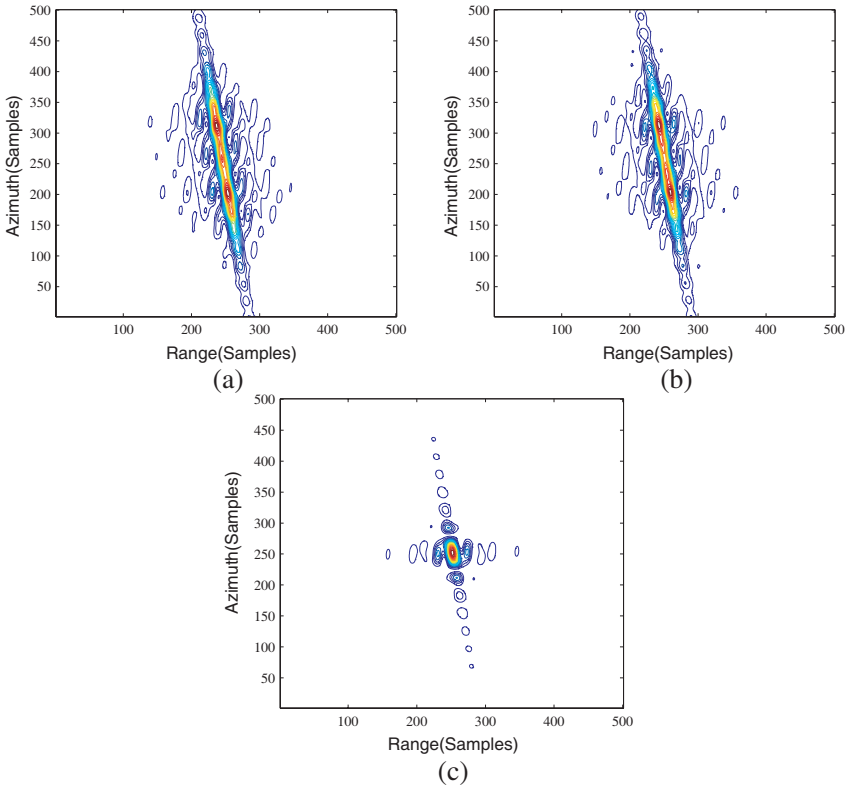

Figure 3. Focusing results of a single point target for case B. (a) OLBF; (b) ELBF; (c) AILBF.

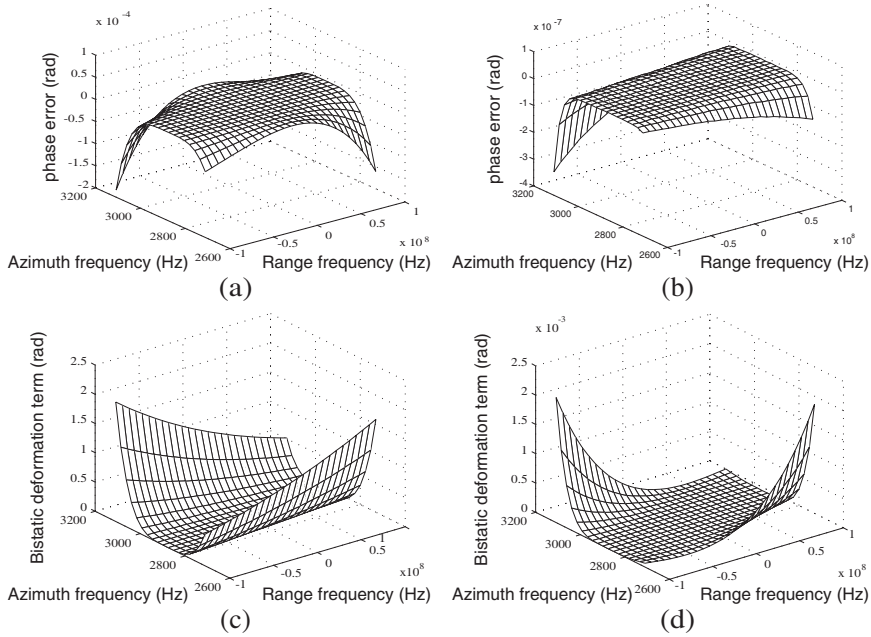

Figure 4. The phase error and BD phase term of AILBF using 1st-order and 2nd-order expansion of the Doppler frequency. (a) Phase error of 1st-order expansion; (b) Phase error of 2nd-order expansion; (c) BD term of 1st-order expansion; (d) BD term of 2nd-order expansion.

5. CONCLUSION

In this paper, the generalized LBF (GLBF), ideal LBF (ILBF) and an approximated ILBF (AILBF) are presented. GLBF supplies us with a general tool to deduce bistatic SAR PTRS, and a theoretical ideal PTRS is given by ILBF. AILBF can be utilized to imaging algorithm development for extreme bistatic and large squint bistatic SAR. The theoretical analysis and simulation results show that AILBF can work well for general bistatic SAR, in comparison with original LBF and extended LBF. Next we will develop the imaging algorithms based on ILBF and AILBF.

ACKNOWLEDGMENT

The authors would like to thank the Associate Editor and the anonymous reviewers, whose suggestions are very valuable in improving the manuscript. This work is supported by the National High-tech Research and Development Program (863

Program) of China (No. 2009AA12Z106), the Pre-research Foundation (No. 9140A07011609DZ0217) and the Fundamental Research Funds for the Central Universities (No. A03006023901007).

REFERENCES

1. Chan, Y. K. and V. C. Koo, "An introduction to synthetic aperture radar (SAR)," *Progress In Electromagnetics Research B*, Vol. 2, 27–60, 2008,
2. Lim, S. H., J. H. Han, S. Y. Kim, N. H. Myung, "Azimuth beam pattern synthesis for airborne SAR system optimization," *Progress In Electromagnetics Research*, Vol. 106, 295–309, 2010.
3. Wei, S. J., X. L. Zhang, J. Shi, and G. Xiang, "Sparse reconstruction for SAR imaging based on compressed sensing," *Progress In Electromagnetics Research*, Vol. 109, 63–81, 2010.
4. Xu, W., P. Huang, and Y. K. Deng, "Multi-channel SPCMB-TOPS SAR for high-resolution wide-swath imaging," *Progress In Electromagnetics Research*, Vol. 116, 533–551, 2011.
5. Wei, S. J., X. L. Zhang, and J. Shi, "Linear array SAR imaging via compressed sensing," *Progress In Electromagnetics Research*, Vol. 117, 299–319, 2011.
6. Liu, Q., W. Hong, W. X. Tan, Y. Lin, Y. Wang, and Y. Wu, "An improved polar format algorithm with performance analysis for geosynchronous circular SAR 2D imaging," *Progress In Electromagnetics Research*, Vol. 119, 155–170, 2011.
7. Ben Kassem, M. J., J. Saillard, and A. Khenchaf, "BISAR mapping I. Theory and modelling," *Progress In Electromagnetics Research*, Vol. 61, 39–65, 2006.
8. Ben Kassem, M. J., J. Saillard, and A. Khenchaf, "BISAR mapping II Treatment, simulation and experimentation," *Progress In Electromagnetics Research*, Vol. 61, 67–87, 2006.
9. Liu, Q., S. Xing, X. Wang, J. Dong, and D. Dai, "A strip-map SAR coherent jammer structure utilizing periodic modulation technology," *Progress In Electromagnetics Research B*, Vol. 28, 111–128, 2011.
10. Krieger, G., H. Fiedler, and A. Moreira, "Bi- and multistatic SAR: Potentials and challenges," *Proc. EUSAR*, 365–370, Ulm, Germany, May 2004.
11. Cumming, I. G. and F. H. Wong, *Digital Processing of Synthetic Aperture Radar Data: Algorithms and Implementation*, Artech House, Norwood, MA, 2005.
12. Chan, Y. K. and Lim, S. Y., "Synthetic aperture radar (SAR)

signal generation," *Progress In Electromagnetics Research B*, Vol. 1, 269–290, 2008.

13. Zhao, Y. W., M. Zhang, and H. Chen, "An efficient ocean SAR raw signal simulation by employing fast Fourier transform," *Journal of Electromagnetic Waves and Applications*, Vol. 24, No. 16, 2273–2284, 2010.
14. Chang, Y. L., C. Y. Chiang, and K. S. Chen, "SAR image simulation with application to target recognition," *Progress In Electromagnetics Research*, Vol. 119, 35–57, 2011.
15. Zhang, M., Y. W. Zhao, H. Chen, and W. Q. Jiang, "SAR imaging simulation for composite model of ship on dynamic ocean scene," *Progress In Electromagnetics Research*, Vol. 113, 395–412, 2011.
16. Wang, X., D. Zhu, and Z. Zhu, "An implementation of bistatic PFA using chirp scaling," *Journal of Electromagnetic Waves and Applications*, Vol. 24, No. 5–6, 745–753, 2010.
17. Guo, D., H. Xu, and J. Li, "Extended wavenumber domain algorithm for highly squinted sliding spotlight SAR data processing," *Progress In Electromagnetics Research*, Vol. 114, 17–32, 2011.
18. Mao, X. H., D. Y. Zhu, L. Ding, and Z. D. Zhu, "Comparative study of RMA and PFA on their responses to moving target," *Progress In Electromagnetics Research*, Vol. 110, 103–124, 2010.
19. Loffeld, O., H. Nies, V. Peters, and S. Knedlik, "Models and useful relations for bistatic SAR processing," *IEEE Trans. Geosci. Remote Sens.*, Vol. 42, No. 10, 2031–2038, October 2004.
20. Sun, J., S. Mao, G. Wang, and W. Hong, "Extended exact transfer function algorithm for bistatic SAR of translational invariant case," *Progress In Electromagnetics Research*, Vol. 99, 89–108, 2009.
21. Sun, J., S. Mao, G. Wang, and W. Hong, "Polar format algorithm for spotlight bistatic SAR with arbitrary geometry configuration," *Progress In Electromagnetics Research*, Vol. 103, 323–338, 2010.
22. Neo, Y. L., F. H. Wong, and I. G. Cumming, "A comparison of point target spectra derived for bistatic SAR processing," *IEEE Trans. Geosci. Remote Sens.*, Vol. 46, No. 9, 2481–2492, September 2008.
23. Neo, Y. L., F. H. Wong, and I. G. Cumming, "A two-dimensional spectrum for bistatic SAR processing using series reversion," *IEEE Geosci. Remote Sens. Lett.*, Vol. 4, No. 1, 93–96, September 2007.
24. Bamler, R., F. Meyer, and W. Liebhart, "Processing of bistatic

SAR data from quasi-stationary configurations," *IEEE Trans. Geosci. Remote Sens.*, Vol. 45, No. 11, 3350–3358, November 2007.

25. Natroshvili, K., O. Loffeld, H. Nies, A. M. Ortiz, and S. Knedlik, "Focusing of general bistatic SAR configuration data with 2-D inverse scaled FFT," *IEEE Trans. Geosci. Remote Sens.*, Vol. 44, No. 10, 2718–2727, October 2006.
26. Wang, R., O. Loffeld, Q. Ul-Ann, H. Nies, A. Medrano Ortiz, and A. Samarah, "A bistatic point target reference spectrum for general bistatic SAR processing," *IEEE Geosci. Remote Sens. Lett.*, Vol. 5, No. 3, 517–521, July 2008.
27. Sew, B. C., Y. K. Chan, C. S. Lim, T. S. Lim, and V. C. Koo, "Modified multilook cross correlation (MLCC) algorithm for Doppler centroid estimation in synthetic aperture radar signal processing," Progress In Electromagnetics Research C, Vol. 20, 215–225, 2011.
28. Choi, G. G., S. H. Park, H. T. Kim, and K. T. Kim, "ISAR imaging of multiple targets based on particle swarm optimization and hough transform," *Journal of Electromagnetic Waves and Applications*, Vol. 23, No. 14–15, 1825–1834, 2009.
29. Tian, B., D. Y. Zhu, and Z. D. Zhu, "A novel moving target detection approach for dual-channel SAR system," *Progress In Electromagnetics Research*, Vol. 115, 191–206, 2011.
30. Walterscheid, I., T. Espeter, A. Brenner, J. Klare, J. Ender, H. Nies, R. Wang, and O. Loffeld, "Bistatic SAR experiments with PAMIR and terraSAR-X: Setup, processing, and image results," *IEEE Trans. Geosci. Remote Sens.*, Vol. 48, No. 8, 3268–3279, 2010.
31. Ul-Ann, Q., O. Loffeld, H. Nies, R. Wang, and S. Knedlik, "Optimizing the individual azimuth contribution of transmitter and receiver phase terms in Loffeld's bistatic formula (LBF) for bistatic SAR processing," *Proc. IGARSS*, Vol. 3, III-455–III-458, 2008.
32. Yang, K., F. He, and D. Liang, "A two-dimensional spectrum for general bistatic SAR processing," *IEEE Geosci. Remote Sens. Lett.*, Vol. 7, No. 1, 108–112, 2010.
33. Wang, R., O. Loffeld, Y. Neo, H. Nies, and Z. Dai, "Extending Loffeld's bistatic formula for the general bistatic SAR configuration," *IET Radar, Sonar & Navigation*, Vol. 4, No. 1, 74–84, 2010.
34. Wu, J., J. Yang, Y. Huang, H. Yang, and H. Wang, "Bistatic forward-looking SAR: Theory and challenges," *Proc. IEEE Radar Conf.*, 1–4, Pasadena, CA, May 2009.